

Synthesis of ZnO-CuO flower-like hetero-nanostructures as volatile organic compounds (VOCs) sensor at room temperature

RAAD S. SABRY, ROONAK ABDUL SALAM A. ALKAREEM*

Department of Physics, College of Science, Al-Mustansiriyah University, Iraq

ZnO-CuO flower-like hetero-nanostructures were successfully prepared by combining hydrothermal and dip coating methods. Flower-like hetero-nanostructures of ZnO-CuO were examined by X-ray diffraction (XRD), field emission scanning electron microscopy (FE-SEM), and UV-Vis. The sensing properties of ZnO-CuO flower-like hetero-nanostructures to volatile organic compounds (VOCs) were evaluated in a chamber containing acetone or isopropanol gas at room temperature. The sensitivity of ZnO-CuO flower-like hetero-nanostructures to VOCs was enhanced compared to that of pure leafage-like ZnO nanostructures. Response and recovery times were about 5 s and 6 s to 50 ppm acetone, and 10 s and 8 s to 50 ppm isopropanol, respectively. The sensing performance of ZnO-CuO flower-like hetero-nanostructures was attributed to the addition of CuO that led to formation of p-n junctions at the interface between the CuO and ZnO. In addition, the sensing mechanism was briefly discussed.

Keywords: *hydrothermal process; dip coating; hetero-nanostructures; volatile organic compounds (VOCs)*

1. Introduction

Volatile organic compounds (VOCs) are organic chemical compounds that have a boiling point less than or equal to 250 °C at 101.3 kPa pressure (EUROPA, 2004) [1]. VOCs contained in air belong to different groups of compounds such as carbonyl compounds (aldehydes and ketones), aromatic hydrocarbons, alcohols, halogenated hydrocarbons, ethers and others. These compounds are sources of consumer products, such as polishes, paints, cleaning products, glues and sealants. These domestic products have caused about 20 % of poisoning incidents and over 80 % of those incidents were accidental child poisonings [2]. Therefore, it is necessary to monitor the concentrations of VOCs in the environment. Continuous interest is directed toward developing the VOCs sensor with rapid response and recovery times and higher sensitivity to determine and control the VOCs in the environment. To verify these goals, a considerable

attention has been focused on the development of VOCs sensitive to nanomaterials due to their high surface to volume ratio [3].

It is known that a favorite gas sensor should have a combination of longterm stability, high sensitivity and selectivity and low operating temperature. These parameters are mainly dependent on crystal structure, effective surface area, additives and defect density [4].

Semiconductor metal oxides as gas sensing materials have been widely studied for a long time due to their beneficial properties, such as simplicity in fabrication, fast response, ease of fabrication, low cost, small size and low detection limits (<ppm level) [5]. For this reason, some semiconductor metal oxide sensors are used as an effective tool to detect pollutant gases and various VOCs [6]. Among semiconductor metal oxides, zinc oxide (ZnO) is one of the premier materials studied as a gas sensor. This is primarily due to the good thermal and chemical stability under operating conditions and also high mobility of conduction electrons in the material [7, 8].

*E-mail: roony19882009@yahoo.com

Table 1. Sensing response behavior of n-type and p-type materials to reducing and oxidizing gases [12].

Sensor response behavior	n-type material	p-type material	Example gases
Reducing gases	Resistance decreases	Resistance increases	H ₂ , H ₂ S, CO, NH ₄ , ethanol, acetone, CH ₄
Oxidizing gases	Resistance increases	Resistance decreases	O ₂ , O ₃ , NO _x , CO ₂ , SO ₂
Dominant charge carrier	electrons (e ⁻)	holes (h ⁺)	–

It is n-type wide band gap semiconductor (3.37 eV), with a large excited binding energy (60 meV), good photochemical properties, non-toxic and inexpensive. Zinc oxide (ZnO) nanostructures are of particular interest for many applications, such as sensors, catalysts, field emitters and solar cells [9, 10]. As another important semiconductor metal oxide, copper oxide (CuO) is a kind of intrinsic p-type semiconductor with a narrow band gap. It has great potential as an active catalyst; it is used in solar cells and in gas sensing [11]. Therefore, introducing CuO may be a more economical and reasonable way to enhance ZnO gas sensing performance.

During n-type material (majority charge carriers are electrons) interaction with a reducing gas, a decrease in resistance occurs. Conversely, an oxidizing gas serves to deplete the sensing layer of electrons resulting in an increase in resistance. P-type materials (majority charge carrier are holes) exhibit reverse behavior as shown in Table 1.

To combine the advantages of the ZnO and the CuO materials and thus to improve the performance of their combination, a flower-like ZnO-CuO hetero-nanostructure has been synthesized and used in this work. ZnO-CuO flower-like hetero-nanostructures were prepared by combining hydrothermal and dip coating methods. Present work investigates the sensitivity of the ZnO-CuO flower-like hetero-nanostructures toward VOCs such as acetone and isopropanol at room temperature.

2. Experimental

2.1. Chemicals

Materials used for preparation included: zinc nitrate hexahydrate (Zn(NO₃)₂·6H₂O, Scharlau,

Spain), copper nitrate trihydrate (Cu(NO₃)₂·3H₂O, BDH), hexamethylenetetramine (HMT, C₆H₁₂N₄, BDH) and sodium hydroxide (97 % to 100 %, NaOH, Scharlau Spain). Distilled water was used throughout the experiments. These materials as well as the measured materials: acetone (99.9 %, C₃H₆O, TEDIA, USA) and isopropanol also called isopropyl alcohol (99.8 %, C₃H₈O, IPA, Ireland) were all used as received.

2.2. Synthesis process

2.2.1. Preparation of ZnO leafage-like nanostructure

Zinc oxide (ZnO) leafage-like nanostructure was synthesized using hydrothermal method. 0.1 M of zinc nitrate hexahydrate and hexamethylenetetramine (HMT) were dissolved in 100 mL distilled water. Then, 0.2 M of NaOH was added to the mixture under slow stirring for 1 hour at room temperature to adjust pH of the solution to the value of 10.6, using BP3001 Professional Benchtop pH Meter.

The prepared solution was transferred to an autoclave in an oven and heated to 110 °C for 5 hours. The obtained white powder was washed several times with distilled water to remove all residues and impurities. Then the prepared powder was added to some amount of distilled water in order to drop it on a substrate (glass or Si wafer) under heating at 50 °C on a hot plate in air.

2.2.2. Synthesis of ZnO-CuO flower-like hetero-nanostructures

Zinc oxide (ZnO) leafage-like nanostructures were prepared by hydrothermal method as described in Section 2.2.1. 80 mL of aqueous solution containing 0.048 wt.% copper nitrate trihydrate and 0.0056 wt.% hexamethylenetetramine (HMT) were transferred into a 100 mL glass

autoclave. Thick films made of ZnO leafage-like nanostructures were dipped in the aqueous solution of copper nitrate under slow stirring for 30 s. After that, the composite copper nitrate/ZnO leafage-like nanostructures were calcined at 500 °C for 1 hour to transform the copper nitrate to CuO through thermal oxidation and obtain ZnO-CuO flower-like hetero-nanostructures.

2.3. Volatile organic compounds (VOCs) sensing

ZnO-CuO flower-like hetero-nanostructures were connected by silver conducting electrode (interdigital electrodes, IDE) using screen printing method. After the electrode deposition, the device was ready for VOCs sensing. The VOCs sensor properties were examined using a home-made testing system. Typically, VOCs sensing measurement was performed in a closed test chamber with an effective volume of 1317.5 cm³ at room temperature. The sensor was placed in the test chamber, and then a given amount of VOCs (acetone or isopropanol) was injected into the chamber by a syringe. The resistance change was monitored by a Keithley 2430 instrument. The sensitivity is defined as:

$$S(\%) = |(R_a - R_g)/R_g| \times 100(\%) \quad (1)$$

where R_a and R_g represent the resistance of the specimen upon exposure to air and gas, respectively [13].

2.4. Characterization

The crystalline structure of the specimen was characterized by X-ray diffraction (XRD, Miniflex II Rigaku, Japan) with $\text{CuK}\alpha$ radiation ($\lambda = 0.15406$ nm). The morphology of the specimen was characterized by field emission scanning electron microscope (FE-SEM, Hitachi-S 4160, Japan) at 15 kV acceleration voltage. Also, UV-Vis measurements of ZnO-CuO flower-like hetero-nanostructures were recorded by using a microprocessor UV-Vis spectrophotometer (Double beam LI-2800).

3. Results and discussion

Fig. 1a and Fig. 1b show the XRD patterns of ZnO nanostructures and ZnO-CuO flower-like hetero-nanostructures, respectively. After synthesis of ZnO-CuO flower-like hetero-nanostructures, three new diffraction peaks were observed at 35.31°, 38.91°, and 49.06°, when compared with pure ZnO nanostructures, which can be attributed to (0 0 2), (2 0 0) and (2 0 2) characteristic peaks of the monoclinic CuO JCPDS Card No. 44-0706, respectively. The peaks at (1 0 0), (0 0 2), (1 0 1), (1 0 2), (1 1 0), and (1 0 3), correspond to hexagonal wurtzite ZnO (JCPDS Card No. 36-1451). The broadening and small peaks of CuO nanostructures can be attributed to the small crystallite size and poor crystallinity of CuO in ZnO-CuO flower-like hetero-nanostructures. No peaks for Cu_2O phase were observed, implying that in the annealing process the copper nitrate completely converted into CuO. Crystallite size was calculated using the Scherrer relation [14]:

$$D = k\lambda / \beta \cos \theta \quad (2)$$

where k is a constant (equal to 0.9 assuming that the particles are spherical), D is the average crystallite size, λ is the X-ray wavelength of 0.15406 nm, θ is the Bragg diffraction angle and β is the full width at half maximum. Compared with pure ZnO nanostructures, the average crystallite size of the ZnO-CuO flower-like hetero-nanostructure determined from (1 0 0) and (1 0 1) diffraction peaks decreased from 19.83 nm to 18.44 nm, which implies that the presence of CuO nanostructures influences the crystallite size to a certain degree. The average crystallite size of CuO is 18.80 nm.

Fig. 2a and Fig. 2b show the FE-SEM images of the ZnO nanostructures (pH = 10.6) at low and high magnifications, respectively. Fig. 2a shows that the specimen has high homogeneity. The pH of the solution is a critical parameter for particle size, phase formation, and morphology of the structure during the solution growth. As observed in Fig. 2b, the ZnO has leafage-like nanostructures, whose morphology depends on the pH value during the solution growth. It is clear that the structure comprises several leafages of about 100 nm

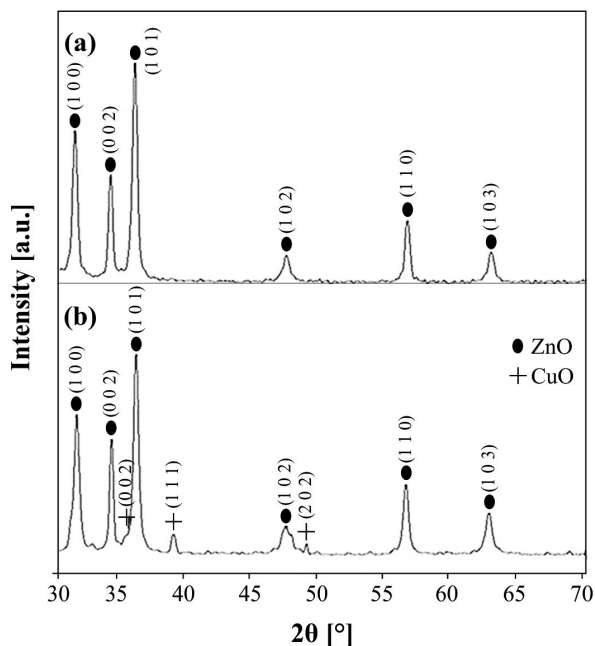


Fig. 1. XRD pattern for (a) ZnO nanostructures, and (b) ZnO-CuO flower-like hetero-nanostructures.

to 700 nm length and about 50 nm to 250 nm thickness. Fig. 2c and Fig. 2d show the morphology of ZnO-CuO flower-like hetero-nanostructures at low and high magnifications, respectively. After dip coating and annealing process of the ZnO nanostructure, the ZnO-CuO flower-like hetero-nanostructures were formed. It can be seen from Fig. 2c that the obtained structure is composed of large quantities of flower-like ZnO-CuO hetero-nanostructures. From the enlarged FE-SEM image in Fig. 2d it is clearly seen that the flower petals exhibit the tapering features with the root size of 100 nm to 300 nm and tip size of 50 nm to 100 nm approximately.

Fig. 3a shows the typical transmittance spectra of ZnO nanostructures. The low transmittance percentage below 360 nm indicates the strong absorbance of ZnO nanostructures in this region, which has higher energy than the energy gap of ZnO semiconductor in UV-Vis range. This blue shift is associated with the decrease in crystallite size, which is consistent with XRD results. The band gap of the ZnO nanostructures is 3.4 eV as shown in Fig. 3b. Fig. 3c shows the optical transmittance of the ZnO-CuO flower-like

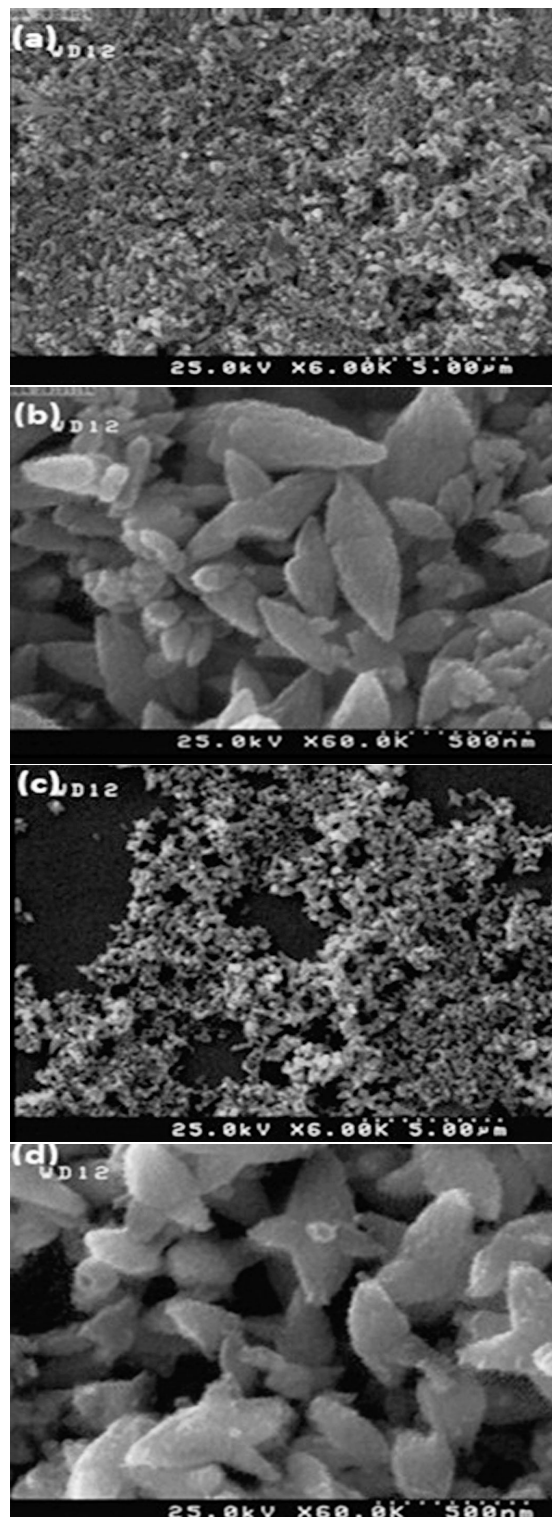


Fig. 2. FE-SEM images of ZnO leafage-like nanostructure (a) low magnification, (b) high magnification, and ZnO-CuO flower-like hetero-nanostructure (c) low magnification, (d) high magnification.

hetero-nanostructures. As observed from Fig. 3c there is a low transmittance below 380 nm indicating the strong absorbance of ZnO-CuO flower-like hetero-nanostructures in this region; the red shift is attributed to small band gap of CuO (1.2 eV to 1.5 eV). The band gap for ZnO-CuO flower-like hetero-nanostructures decreased from 3.4 to 3.1 eV compared with pure ZnO nanostructures as shown in Fig. 3d.

Fig. 4a and Fig. 4b show the transient resistance response of pure ZnO nanostructures and ZnO-CuO flower-like hetero-nanostructures upon exposure to 50 ppm, 100 ppm and 150 ppm of acetone and isopropanol at room temperature, respectively. It is clear that the resistance of ZnO nanostructures and ZnO-CuO flower-like hetero-nanostructures initially shows a rapid decline followed by slow decay after injecting VOCs (acetone or isopropanol). However, the resistance rises very fast with time when VOCs was exhausted from the chamber and air was inserted. ZnO-CuO flower-like hetero-nanostructures show n-type gas sensing behavior, that is, the resistance decreases in response to exposing to acetone and isopropanol. The contact of two different types of metal oxide semiconductors results in the formation of p-n junctions at the interface between the CuO and ZnO, leading to the decrease in resistance of ZnO-CuO flower-like hetero-nanostructures compared with the pure ZnO.

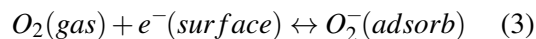
The sensitivity of the pure ZnO leafage-like nanostructure and ZnO-CuO flower-like hetero-nanostructure to different concentrations of acetone and isopropanol (50 ppm, 100 ppm, 150 ppm) at room temperature is shown in Fig. 4c and Fig. 4d, respectively. As observed, the sensitivity to acetone shows higher response compared with isopropanol at room temperature. The sensitivity magnitude is based on the molar volume and the ppm concentration of the VOCs. The molar volume of acetone and isopropanol were 73.42 cm³/mol and 76.46 cm³/mol, respectively. The small molar volume indicates that the molecules can easily diffuse into and effuse out of the specimen [15]. From Fig. 4c and Fig. 4d it can be seen that the ZnO-CuO flower-like hetero-nanostructure

exhibits higher sensitivity than that of pure ZnO leafage-like nanostructure in the whole testing range. Table 2 illustrates the response and recovery time of ZnO nanostructures and ZnO-CuO flower-like hetero-nanostructures. For acetone at the levels of 50 ppm, 100 ppm, 150 ppm, the sensitivities are about 13.02 %, 20.21 %, 43.06 % for ZnO nanostructures and 14.19 %, 24.34 %, 54.96 % for ZnO-CuO flower-like hetero-nanostructures, respectively.

According to Maziarz et al. [16], the enhanced sensitivity and response time of SnO₂-decorated flower-like TiO₂ 3D nanostructures can be attributed to the structure of the sample and using high temperature (308 °C) during the sensing measurements.

Our work shows that the ZnO-CuO flower-like hetero-nanostructures are characterized by enhanced response and recovery times and also increased sensitivity (compared with pure ZnO nanostructures) at room temperature due to the high aspect surface to volume ratio of the structure which provides many sites to adsorb and desorb gas molecules and also possibility of forming numerous p-n heterojunctions at the interface between CuO nanoparticles and ZnO leafage-like nanostructures.

The principle of metal oxide gas sensor mainly depends upon oxygen concentration and its rate of adsorption and desorption. The adsorption can be enhanced by increasing the operating temperature, reducing the grain size, and using dopants. Below the temperature of 200 °C, oxygen molecules in the atmosphere are adsorbed on the sensor surface and form the oxygen ion molecules by attracting an electron from the conduction band of metal oxide semiconductor as shown in the following equation [17]:



Typically, the sensing mechanism of ZnO is based on gas adsorption and desorption on the surface of ZnO. When the ZnO nanostructures sensor is exposed to air, oxygen from the air can be adsorbed on the surface of the ZnO nanostructures

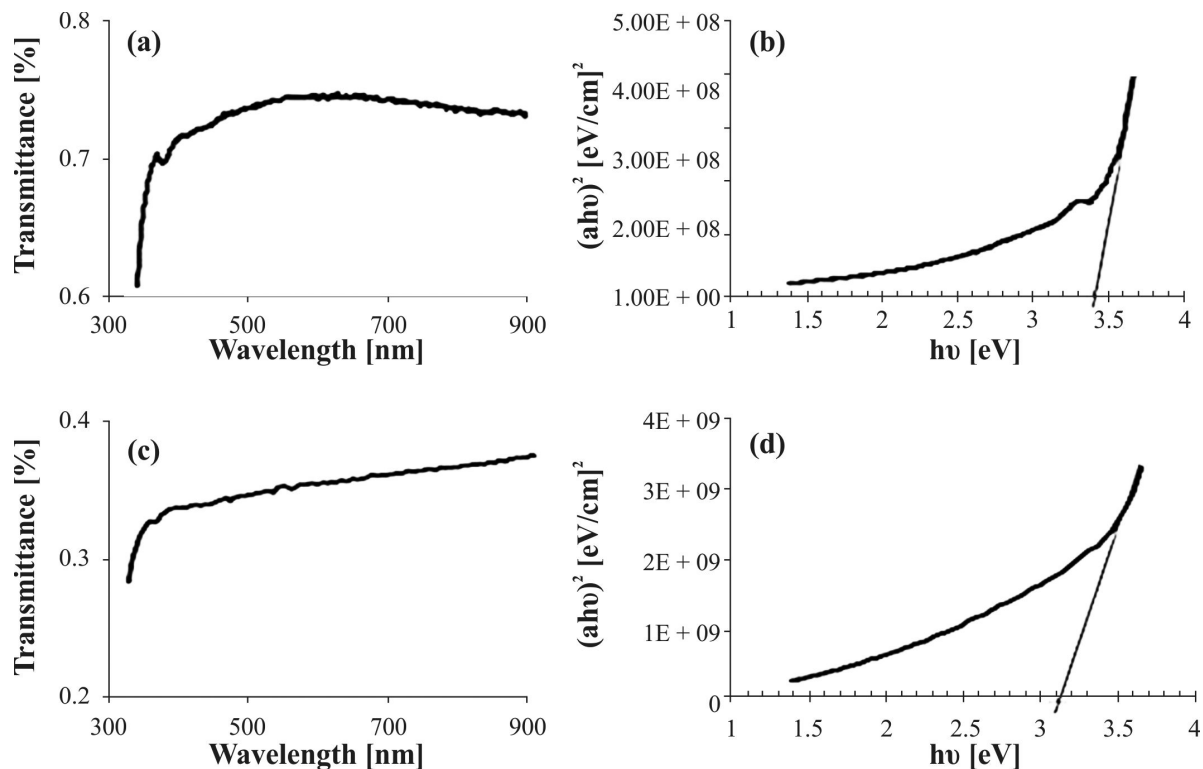


Fig. 3. Transmittance curves for (a) ZnO nanostructure and (c) ZnO-CuO flower-like hetero-nanostructure, $(\alpha h\nu)^2$ vs. photon energy for (b) ZnO nanostructure and (d) ZnO-CuO flower-like hetero-nanostructure.

and extract electrons from the conduction band of ZnO nanostructures to form O_2^- , which can produce a depletion layer on the surface of the nanostructures and result in an increase in sensor resistance [18]. When a ZnO sensor containing nanostructures is exposed to reductive gases at room temperature, such as acetone or isopropanol vapors, the negative oxygen on surface can react with the reductive gas molecules and release electrons back to the conduction band of ZnO nanostructures, leading to a decrease in resistance of the sample. The sensing mechanism of ZnO-CuO flower-like hetero-nanostructure is somewhat different due to the formation of p-n heterojunctions. In air, oxygen molecules capture electrons from CuO NPs, and chemisorbed oxygen O_2^- molecules are formed on ZnO-CuO hetero-nanostructure surface. Meanwhile, electrons transfer from ZnO to CuO resulting in formation electron depletion layer extending into ZnO [19]. Upon exposure to acetone or isopropanol, the gas molecules react with chemisorbed oxygen O_2^- and electrons are released

to CuO. Then, the electrons return from CuO to ZnO, leading to the reduction of electron depletion layer thickness, and consequently, the decrease in resistance of ZnO-CuO hetero-nanostructures. This can be the operating mechanism of the ZnO-CuO flower-like hetero-nanostructures for acetone and isopropanol sensing.

Up to date, many researches have reported on the p-n semiconductor nanostructures used as gas sensors with high operating temperature. In this work, ZnO-CuO flower-like hetero-nanostructures exhibited high sensitivity and short response and recovery times to VOCs vapor, which might provide an alternative strategy to improve the VOCs sensing properties of semiconductor nanostructures at room temperature.

4. Conclusions

In conclusion, pure ZnO nanostructures and ZnO-CuO flower-like hetero-nanostructures were synthesized by combining hydrothermal and dip

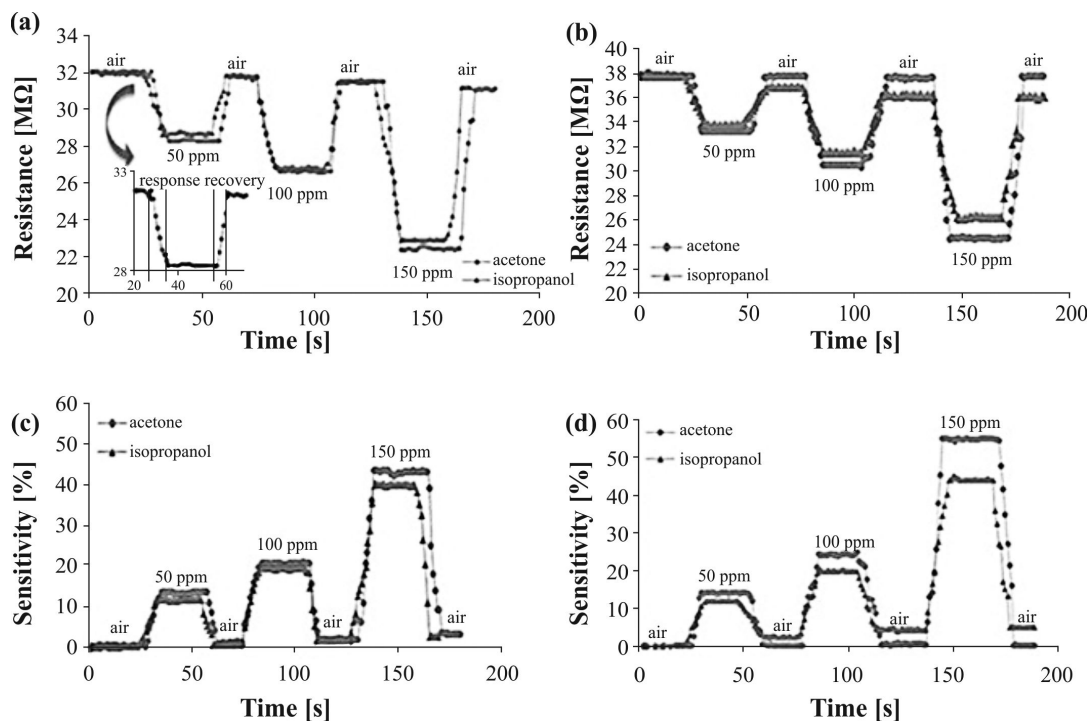


Fig. 4. Transient resistance response of: (a) ZnO nanostructures (the inset shows response and recovery time for acetone at 50 ppm), (b) ZnO-CuO flower-like hetero-nanostructures; sensitivity of: (c) ZnO nanostructures, and (d) ZnO-CuO flower-like hetero-nanostructures.

Table 2. Response and recovery time of ZnO nanostructures and ZnO-CuO flowers like hetero-nanostructures.

Preparation condition	Response time [s]		Recovery time [s]	
Acetone				
Zn nanostructures	50 ppm	8	50 ppm	5
	100 ppm	9	100 ppm	5
	150 ppm	10	150 ppm	7
Zn-CuO flower-like hetero-nanostructures	50 ppm	5	50 ppm	6
	100 ppm	8	100 ppm	12
	150 ppm	10	150 ppm	11
Isopropanol				
Zn nanostructures	50 ppm	9	50 ppm	6
	100 ppm	10	100 ppm	6
	150 ppm	11	150 ppm	8
Zn-CuO flower-like hetero-nanostructures	50 ppm	10	50 ppm	8
	100 ppm	11	100 ppm	10
	150 ppm	13	150 ppm	11

coating methods. Their structural, morphological, optical as well as sensing performance were investigated. Sensing performance of the ZnO nanostructures shows good sensitivity

to VOCs at room temperature. For the same concentration of VOCs, ZnO-CuO flower-like hetero-nanostructures show the highest sensitivity. The enhanced sensitivity and quick

response/recovery time of these heterostructures at room temperature are explained by the formation of p-n heterojunction between CuO NPs and ZnO nanostructures. In addition, the high aspect surface to volume ratio provides more active sites to adsorb and desorb the gas molecules. Also, the decoration of CuO NPs promotes the chemical reactions and the chemisorption of oxygen species on the surface of ZnO-CuO flower-like hetero-nanostructure. The results demonstrate the potential application of ZnO nanostructures and ZnO-CuO flower-like hetero-nanostructures for fabricating high performance VOCs sensors at room temperature.

References

- [1] DINH T., CHOI I., SON Y., SONG K., SUNWOO Y., KIM J., *J. Environ. Manage.*, 168 (2016), 157.
- [2] HUZAR E., WONDNICKA A., DZIECIOŁ M., *Ecol. Chem. Eng. A*, 18 (2011), 991.
- [3] GAVGANI J., DEHSARI H., HASANI A., MAHYARI M., SHALAMZARI E., SALEHI A., TAROMI F., *RSC Adv.*, 5 (2015), 57559.
- [4] HOSSEINI Z., IRAJIZAD A., MORTEZAALI A., *Sensor. Actuat. B-Chem.*, 207 (2015), 865.
- [5] KANAN S., EL-KADRI O., ABU-YOUSEF I., KANAN M., *Sensors*, 9 (2009), 8158.
- [6] LEONARDI S., *Chemosensors*, 5 (2017), 1.
- [7] HUANG X., CHOI Y., *Sensor. Actuat. B-Chem.*, 122 (2007), 659.
- [8] PANDYA H., CHANDRA S., VYAS A., *Sensor Devices*, (2011), 69.
- [9] ALLAF R., HOPE-WEEKS L., *J. Nanomater.*, 2014 (2014), 1.
- [10] RAMIREZ A., RAMIREZ I., ILIANA (Eds.), *Photocatalytic semiconductors: synthesis, characterization, and environmental applications*, Springer, New York, 2015.
- [11] TRAN T., NGUYEN V., *Int. Sch. Res. Notices*, (2014), 1.
- [12] DEREK R., SHEIKH A., PATRICIA A., *Sensor. Actuat. B-Chem*, 204 (2014), 250.
- [13] CHOWA L., LUPANA O., CHAI G., KHALLAF H., ONO L., ROLDAN C., TIGINYANU I., URSAKI V., SONTE V., SCHULTE A., *Sensor. Actuat. A-Phys*, 189 (2013), 399.
- [14] ABBAS K., BIDIN N., SABRY R., AL-ASEDY H., AL-AZAWI M., ISLAM S., *Mater. Chem. Phys.*, 182 (2016), 298.
- [15] CHOI J., PARK D.W., SHIM S.E., *Synthetic Met.*, 162 (2012), 1513.
- [16] MAZIARZ W., KUSIOR A., ZAIAC A.T., *Beilstein J. Nanotech.*, 7 (2016), 1718.
- [17] SHANKAR P., BALAGURU RAYAYAPPAN J.B., *Science Jet*, 4(2015), 1.
- [18] AL-HARDAN N., ABDULLAH M., ABDUL AZIZ A., AHMAD H., LOW L., *Vacuum*, 85 (2010), 101.
- [19] CHEN Y., SHEN Z., JIA Q., ZHAO J., ZHAO Z., JI H., *Roy. Soc. Chem.*, 6 (2016), 2504.

Received 2017-07-19

Accepted 2018-05-02